

BIOINSPIRED SIMULATION OF KNOTTING HAGFISH VIA THIGMOTAXIC INVERSE
DYNAMICS

A Thesis

by

YURA HWANG

Submitted to the Office of Graduate and Professional Studies of
Texas A&M University
in partial fulfillment of the requirements for the degree of
MASTER OF SCIENCE

Chair of Committee, Shinjiro Sueda
Committee Members, John Keyser
Ergun Akleman
Head of Department, Scott Schaefer

December 2019

Major Subject: Computer Science

Copyright 2019 Yura Hwang

ABSTRACT

Hagfishes are capable of not only forming knots, but also sliding them along the length of their bodies. This remarkable behavior is used by the animal for a wide variety of purposes, such as feeding and manipulation. Clearly of interest to biologists, this knotting behavior is also relevant to other fields, such as bioinspired soft robotics. However, this knot-sliding behavior has been challenging to model and has not been simulated on a computer. In this thesis, we present the first physics-based simulation of the knot-sliding behavior of hagfish. We show that a contact-based inverse dynamics approach works well for this challenging control problem, motivated by the biological concept called “positive thigmotaxis,” the characteristics of organisms to be in direct contact with other objects in the local environment.

ACKNOWLEDGMENTS

I would like to thank my adviser Dr. Shinjiro Sueda for his teaching and guidance, my committee members Dr. John Keyser and Dr. Ergun Akleman for their helpful advice, collaborators in Valdosta State University, Dr. Theodore A. Uyeno and Emily E. Evans, for providing hagfish data for our research, my friends in A&M, for their encouragements and inspirations, my brother Inhak, for being my gadfly (Yes, I'm using your favorite Socrates metaphor!), and my parents, who taught me courage and kindness, and provided unlimited support.

CONTRIBUTORS AND FUNDING SOURCES

Contributors

This work was supported by a thesis committee consisting of Professor Shinjiro Sueda of the Department of Computer Science and Engineering, Professor of the Computer Science and Engineering, and Professor Ergun Akleman of the Department of Visualization.

The collection and analysis of data for Chapter 3 was provided by Professor Theodore A. Uyeno, Emily E. Evans, and Austin Haney of Department of Biology at Valdosta State University. Austin Haney helped recording the video of knotting Pacific hagfish, and Emily E. Evans helped in measuring the hagfish flexibility. Washington Department of Fish and Wildlife officer Donna Downs procured the hagfish. These were in part published in year 2017, 2018, and 2019.

All other work conducted for the thesis was completed by the student independently.

Funding Sources

Graduate study was supported in part by the National Science Foundation (IOS-1354788 to T.A.U. and CAREER-1846368 to S.S.).

NOMENCLATURE

q	Generalized position
\dot{q}	Generalized velocity
f	Force vector
h	Time step
λ	Lagrange multiplier vector
M	Mass matrix
K	Stiffness matrix
D	Damping matrix
G	Jacobian of bilateral constraint
C	Jacobian of unilateral constraint
i, j	Colliding body indices in contact handling
a, b	Colliding body indices in contact-based inverse dynamics
s_i, s_j	Spline parameters along the curve
$x(s_i), x(s_j)$	Positions along the curve
$x'(s_i), x'(s_j)$	Tangents along the curve
t_a, t_b	Unit tangent vector
v_a, v_b	Scalar parameters for contact-based inverse dynamics

TABLE OF CONTENTS

	Page
ABSTRACT	ii
ACKNOWLEDGMENTS	iii
CONTRIBUTORS AND FUNDING SOURCES	iv
NOMENCLATURE	v
TABLE OF CONTENTS	vi
LIST OF FIGURES	viii
LIST OF TABLES.....	x
1. INTRODUCTION.....	1
2. BACKGROUND	5
2.1 Knotting Behavior of Hagfish	5
2.2 Cable and Rod Simulation	5
2.3 Neural Control.....	6
3. BIOMETRIC DATA COLLECTION	8
3.1 Hands-on Measurement	8
3.1.1 Volume measurement	8
3.1.2 Twisting Measurement	9
3.2 Photographic Analysis	10
3.3 Kinematic Video Analysis	11
3.3.1 Rules for Knotting	12
4. SIMULATOR.....	13
4.1 Simulation Model	13
4.2 Constraints.....	13
4.2.1 No Constraints	14
4.2.2 Only Bilateral Constraints	15
4.2.3 Bilateral and Unilateral Constraints	15
4.3 Contact Handling.....	16
4.3.1 Collision Detection	16

4.3.2	Newton’s Method.....	16
5.	CONTROLLER	18
5.1	Knot Forming	18
5.2	Knot Sliding Problem	18
5.2.1	Contact-Based Inverse Dynamics.....	19
5.2.1.1	Computations	20
5.2.1.2	Knot Controls.....	21
5.2.1.3	Positive Thigmotaxic Force	23
6.	RESULTS.....	24
6.1	System Configuration	24
6.2	Knot Sliding	24
6.3	Analysis of Force.....	24
7.	CONCLUSION.....	28
7.1	Contributions	28
7.2	Future Work	28
	REFERENCES	30

LIST OF FIGURES

FIGURE	Page
1.1 The knotting behavior of hagfish.	1
3.1 Volume measurement.	9
3.2 Hagfish consisting of 5 segments.	10
3.3 Twisting and bending measurement.	10
3.4 Hagfish video in restraint device [1].	11
4.1 Hagfish model using rigid bodies [1].	14
4.2 Hagfish bodies connected with revolute joints and universal joints [1].	14
4.3 The representation of constraints.	15
4.4 Contact handling [1].	16
4.5 Newton's method [1].	17
5.1 Force applied on the terminal body [1].	19
5.2 The knot forming steps [1].	19
5.3 Real-world knot sliding experiment.	20
5.4 Visual representation of contact-based inverse dynamics [1].	21
5.5 Applying thigmotaxic constraints.	21
5.6 Thigmotaxic constraints for hagfish [1].	22
5.7 Knot tightening.	22
5.8 Knot loosening.	22
6.1 Comparison between our knotting hagfish with <i>positive thigmotaxis</i> and the actual hagfish video [1].	25
6.2 The visual representation of graph coordinates.	25

6.3 The thigmotaxic force becomes zero [1]. 26

LIST OF TABLES

TABLE	Page
3.1 Parameters for simulation.	9
5.1 Scalar parameter values for knot tightening and loosening [1]	20
6.1 Biometric data and inverse dynamics parameters [1].	26

1. INTRODUCTION*

Hagfishes are slime producing marine fish that commonly inhabit the ocean depths. They have incredible flexible bodies, which is best demonstrated by their abilities to tie their bodies to form knots and slide the knots along their bodies. Figure 1.1 shows this behavior. Several purposes for this behavior are described in the literature: they clean slime off their bodies [2]; extricate themselves from narrow spaces or avoid predators [3, 4]; and leverage retractile force to tear off chunks of food during feeding events [5].



Figure 1.1: The knotting behavior of hagfish.

The enhancement of feeding through leverage produced by knotting behavior is important, because hagfishes are *agnathans*, a primitive class¹ of jawless fish. Hagfishes evolved prior to the evolution of vertebrate jaws [6]. Nevertheless, hagfishes can remove considerable morsels while scavenging carcasses. To achieve this, hagfish first embeds the teeth of an eversible toothplate into the food item, such as decaying carcasses of whales. Next, it forms a knot around the tail, and

*Reprinted by permission from Springer Nature Customer Service Center GmbH: Springer Nature, Bioinspired simulation of knotting hagfish [1], 2019. Copyright 2019 Springer Nature Switzerland AG.

¹Technically, a superclass.

slides it anteriorly until a loop of a knot passes over the hagfish's head. The loop is pressed up against the food item, leveraging a powerful retractile force to tear out the morsel [7, 8].

Along with water snakes and eels, hagfishes are one of the three groups of aquatic craniates that manipulate body knots [6, 8, 7]. Interestingly, unlike the others, which form relatively simple knots, hagfishes are capable of tying a diversity of more complicated knots [9].

Hagfishes have shown extensive adaptations for creating and manipulating body knots. These include:

1. Hagfishes do not have hard bones.² Instead of vertebrae, a notochord, which is a flexible, cartilaginous rod, extends down the length of the body and accounts for the majority of the passive body stiffness [10]. It is assumed the core musculature forms a muscular hydrostat that accounts for some of the active body stiffness.
2. The length of the hagfish body is typically over twenty times its width [6]. This extremely elongated body enables the animal to knot itself into a knot.
3. Hagfish has extremely baggy, loose skin. The skin is loosely connected to the musculature of the body wall, precluding tough skin. This enables more room for body maneuvers.
4. The hagfish skin lacks the outer layer, known as the stratum corneum, that produces scales [11, 12]. This enables the animal to retain its smooth skin. Also, hagfishes have no fins or other projections protruding from their bodies that may hinder their knot manipulations.

The hagfish body can be modeled as a large number of body segments connected with joints. The neural inputs increase as the number of joints increases. Theoretically, this requires an enormous amount of neural input, and such models and organisms are described as "hyper-redundant." Neurally controlling such flexibility represents a problem, and the control of this flexibility has been poorly understood by biologists [13, 14]. As a result, researchers have not only struggled with discovering how hagfishes manipulate their bodies during the knot manipulation process, but

²Whether hagfishes were naturally invertebrate animals or vertebrate were lost during evolution, is still a controversial topic.

also with developing a computer simulation of knotting that is realistic and biologically informative.

Our key idea for developing a realistic hagfish simulation is based on a biological concept called “positive thigmotaxis.” Positive thigmotaxis describes a characteristics of organisms to be in direct physical contact with other objects in the local environment.³ From our collaborating marine biologists’ observations, hagfishes also showed positive thigmotaxis. These animals prefer to be pressed up against the edges or by others, rather than being alone. This trait may be due to their poor eye sight. Although they have eye spots, hagfishes’ eyes are covered with tissue, which make them virtually blind to its surroundings. They live in shallow burrows or crevices in the dark zones of the ocean, or prefer to be tightly packed into cavities of whale carcasses [15, 4].

The positive thigmotaxic trait is more evident during the knot manipulation process. While analyzing high speed videos of knotting hagfish, Haney [6] observed that hagfish exhibited positive thigmotaxis during knot formation and manipulation. He also noticed that the types of knots that hagfish can form depend on the number of body crossovers of the tail [16]. Interestingly, while hagfish slides a given knot anteriorly or posteriorly along the body, the constituent crossovers, which indicates places of crossing from one side to the other, did not change in relation to each other. Motivated by this observation, we devised our contact-based inverse dynamics approach.

In this thesis, we present a novel graphics testbed for simulating a knotting hagfish that is biologically informative. Our work has the following contributions.

1. While there are previous works on *knot tying*, there are no previous works related to *knot sliding*. This makes our work the first demonstration of the knot forming and *sliding* behavior.
2. We provide a simulation that is biologically informative to researchers. Often, it is difficult to experiment with real hagfishes in their natural environment. This is due to their natural habitat deep down in the oceans, and the complex procurement process. We used biometric

³Negative thigmotaxis is the opposite characteristic of wanting to be away from others.

data that were collected from real-world hagfish, creating a simulation that biologists may easily understand and use in experiments.

3. Our work is significant in that it has many possible applications areas, most notably, in soft robotics [17]. One of the greatest tasks in current soft robotics research, is in controlling the flexibility and pliancy of robots. We hope our work in knot control would further help in designing and constructing more useful soft robots.

This thesis is organized as follows. In Chapter 2, the related works and background are presented, which is largely divided into 3 main groups: knotting behavior of hagfish; previous works in computer graphics regarding rods and cables; and neural control problems in robotics. In Chapter 3, we explain how the biometric data of real hagfish were collected, and the observations on hagfish knot manipulation. The data was collected by our collaborators, using hands-on measurements, and analyzing photographs and kinematic video. Based on collected data, Chapter 4 explains how we have created our simulation model. We use rigid bodies connected with joints. Both bilateral and unilateral constraints are used to match the hagfish experiment video. In Chapter 5, we present our novel method in knot sliding, *contact-based inverse dynamics*, inspired by positive thigmotaxis. Our approach uses contacts as signals to make the bodies slide. We cast this as a positive thigmotaxi⁴ constraint to our model. Our method enables us to control the knot freely, such as tightening or loosening the knot. It is very simple, easy to use, and computationally efficient. In Chapter 6, we present our results. Our contact-based approach proved to be effective, where sliding motion was incredibly smooth and realistic. Also, from the positive thigmotaxi force, we show several important observations that may be an important clue in finding out hagfish muscle controls. Finally in Chapter 7, we conclude the thesis, by presenting our contributions and future works.

⁴Thigmotaxi is the adjectival form of thigmotaxis.

2. BACKGROUND*

2.1 Knotting Behavior of Hagfish

The knotting behavior of hagfish has been one of the key interests to biologists for a long time. One of the documents for this behavior was done by Adam [2]. By observing *Myxine glutinosa*, or Atlantic hagfish, Adam described how hagfish formed a knot to clean slime off from its body. He also observed that the direction of the knot sliding can be reversed. In other words, the hagfish knot can slide both toward the head, or toward the tail [2]. Ever since this discovery, previous works on hagfish knotting mainly focused on adaptive benefits of the knotting behavior for their survival. These involved hagfishes using their knots to extricate themselves from burrows, escape from predators, pull preys out of holes in active predation, and break large chunks of food in feeding events [5, 7, 8, 4].

The emergence of works that looked into the biomechanisms of this knotting hagfish is relatively a recent phenomenon. Haney [6] not only organized rules for hagfish knotting, but also focused on different kinds of knots that hagfish can formulate. He observed that hagfishes are capable of forming not only simple overhand knots, but also other more complex knots, such as those of figure-8 or Miller-Institute.

While works of Haney mainly involved observing the knotting behavior, Evans et al. [18] analytically examined the hagfish body flexibility using biometric data collected from real-world hagfish. They quantified three-dimensional whole body flexibility of hagfish for applications in virtual simulations. They discovered that the flexibility trend may vary depending on views and skinning. Our simulation used their observations and biometric data in knotting behavior of hagfish.

2.2 Cable and Rod Simulation

Hagfish has a thin, elongated body that resembles rods or cables. There exist numerous approaches for rods and cables in computer graphics, particularly in those of rigid body dynamics

*Reprinted by permission from Springer Nature Customer Service Center GmbH: Springer Nature, Bioinspired simulation of knotting hagfish [1], 2019. Copyright 2019 Springer Nature Switzerland AG.

[19, 20, 21, 22, 23, 24]. In classical work of Baraff, he presents efficient method for computing contacts and frictions on rigid bodies [25]. Other works involved combining rigid and deformable bodies [26, 27, 28, 29, 30]. In our work, we used only rigid degrees of freedom, and deformed the skin mesh using splines for contact handling.

For our simulator, we used the REDMAX method by Wang et al. [30]. REDMAX is a hybrid model that is built using a combined reduced/maximal coordinates. The method is flexible and efficient, and is highly effective for our hagfish simulation. Since hagfish possesses a smooth skin, we exclude friction from our scope [31].

Several works were devoted for simulating knot tying. Phillips et al. [32] proposed a rope tying system that can be used as a surgical simulator for medical surgeons. The rope was created using a spline of linear springs. Focusing on real-time simulation, Brown et al. [33] proposed a simulator in tying virtual, arbitrary knots. The knot tying process involved tying a knot around other objects, with contact and friction along the objects. However, previous systems focused mainly on *knot tying*, not *knot sliding*. Our work is different, in that we have come up with a method in knot sliding simulation, which none of the previous physics-based approach made an attempt at.

2.3 Neural Control

The hagfish body has an extreme flexibility that represents a neural control challenge. If we represent our hagfish model as body segments connected with joints, it requires an enormous amount of neural inputs to control flexibility. This *hyper-redundancy* problem becomes more severe as the number of joints increases [6].

Although poorly understood by biologists in the past, several studies have begun to look into this problem. This trend is most evident in robotics. Sumbre et al. [34] presented a motor primitive of an octopus reaching its arm toward a 3D target point. These motor primitives may adapt to the local environment. For example, when an octopus encounters a narrow hole, the motor primitives would adapt to the constraint, enabling the octopus to successfully reach out through the narrow space.

Motivated by biology, roboticists have worked on designing and constructing soft robots [17,

35, 13]. Soft robots are made of pliant materials, capable of adapting to their surroundings. Controlling such flexibility and pliancy of robots is one of the most difficult tasks that soft robots face. We expect our method to aid in designing and constructing more flexible and efficient soft robots.

Control signals are also of interest to the biomechanics and computer graphics communities. In biomechanics, computed muscle controls were used to control signals of skeletal animals [36]. Similar methods have been proposed in computer graphics, such as controlling humanoids or human hands [37, 38]. However, previous works in neural controls did not consider knot forming or sliding, which is our primary focus.

3. BIOMETRIC DATA COLLECTION*

The biological data measurements for hagfish flexibility were performed by our collaborators in the Department of Biology at Valdosta State University [18, 6]. Although measuring the animal's bending flexibility using curvature was done by our collaborators at Valdosta State University, measuring bending limits in degrees was done by us through photographic analysis on images provided to us by our collaborators. Mostly, our simulation is based on their data and observations. For example, joint stiffness and damping was adjusted by us to approximate the behavior as much as possible. The manually adjusted parameters are listed in Table 6.1.

3.1 Hands-on Measurement

There are various species of hagfish, but for our experiment, *Eptatretus s toutii*, or Pacific hagfish, was chosen. Our collaborators used 4 specimens, which were labeled as *ES102*, *ES103*, *ES104*, and *ES105*. The specimens were euthanized for measurement. For our specific hagfish simulation, data collected from specimen *ES103* was used. The data of other specimens were indirectly used, such as the average twisting limit of the rest of the specimens. The complete list of the data can be found in Chapter 6.

3.1.1 Volume measurement

Unlike mass or length that can be obtained by direct measurement, our collaborators needed to perform volume measurement with care, because it was difficult to measure the hagfish volume directly. They divided the body length into 5 major segments with equal lengths. As can be seen in Figure 3.1, the hagfish was marked in 20% increments in length, resulting in marks at 20%, 40%, 60%, and 80%.

Then, they assumed a simplified hagfish model consisting of 5 cylindrical objects (Figure 3.2). By measuring the circumference of each marked area, the radius was deduced to compute the

*Reprinted by permission from Springer Nature Customer Service Center GmbH: Springer Nature, Bioinspired simulation of knotting hagfish [1], 2019. Copyright 2019 Springer Nature Switzerland AG.

Table 3.1: Parameters for simulation.

Data	Values	Unit
Bending stiffness (Universal)	1e-5	Ncm/rad
Bending stiffness (Revolute)	5e-5	Ncm/rad
Damping	1e-6	$Ncm/rad/s$



Figure 3.1: Pacific hagfish (*Eptatretus stoutii*) was marked with 20% increments in length to measure the approximate volume.

volume of each cylinder. It should be noted that the measurement of the circumference at the 40% mark, and the subsequent values depending on it, may contain a slight error. This is due to the decay of the hagfish skin around that region. However, since the decay was limited to a small range, the effect of the error on the final outcome is almost negligible.

3.1.2 Twisting Measurement

Longitudinal twisting limit data was collected by measuring the twist with the fixation of head and tail, as shown in Figure 3.3. The twisting limit was measured for the *whole*, and the *skinned*. *Whole* refers to a hagfish with its skin attached, and *skinned* refers to a hagfish with its skin removed. The thickness of removed skin consisted of a few millimeters. The purpose was to test whether there existed any influence of skin on hagfish body flexibility. Overall, the *skinned* hagfishes showed larger twisting flexibility, compared to the *whole* ones.

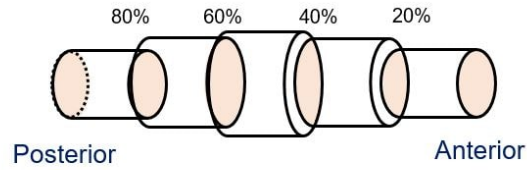


Figure 3.2: Hagfish body was simplified as a model which consists 5 cylindrical objects.

During the experiment, twisting limit data was not collected for *ESI03*. Therefore for the simulation, average *whole* twisting limit for the other 3 specimens were used instead. Nonetheless, based on the skinned body measurement data, it was safely assumed that average data was applicable, since the differences among specimens was not large.

3.2 Photographic Analysis

The bending limit data were not collected at the time of the hands-on experiment. Therefore this step was a post-hoc work, by using the means of analyzing photographs (Figure 3.3). Each specimen was photographed on a copystand using a Sony $\alpha 7s$ digital camera. It displayed dorsal, ventral, and lateral bending. For our simulation, only the ventral bending data were used.

Before collecting the bending data from photographs, they analyzed the overall bending flexibility of hagfishes using the curvature of a circle with radius R . Then, the curvature κ can be

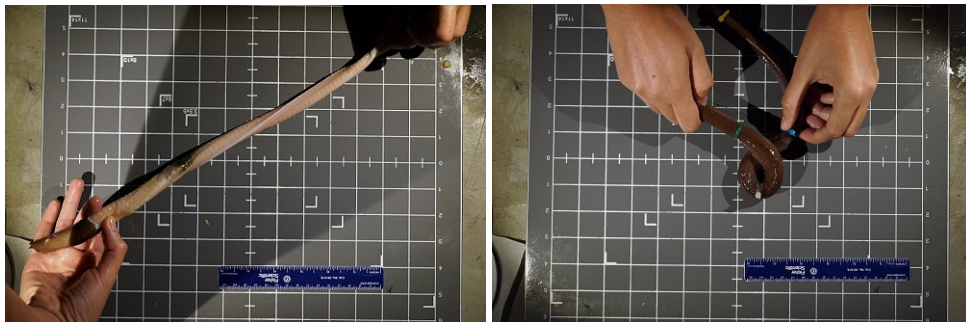


Figure 3.3: Twisting and bending measurement.

deduced using the following property:

$$\kappa = \frac{1}{R}. \quad (3.1)$$

With an image processing tool *FIJI* (ImageJ implementation)¹, they first found the best fitting circle within the marked area of the hagfish body curve. Next, by using the radius of that circle, they generated κ to see the relation of axis and flexibility [18]. The κ was used for analyzing the flexibility, for helping us in choosing bending views. For the actual bending limit in degrees for our simulation, we used a virtual protractor tool.

3.3 Kinematic Video Analysis



Figure 3.4: Hagfish video in restraint device [1].

It is a challenging task to observe and experiment with the knotting behaviors of hagfishes in the natural environment, due to their native habitats in the deep sea. Therefore it is imperative to design a hagfish restraint device, which facilitates controls over consistent hagfish knotting behaviors. Haney created a custom restraint water tank, with a membrane with a hole on one side of the tank [6] (Figure 3.4).

The membrane was used to fix the hagfish's head while it is sedated. Once the anesthesia wears

¹<https://fiji.sc/>

off, the hagfish would attempt to escape from the fixed membrane by knotting and leverage a force on the plate wall. This enabled us to observe the hagfish's knotting in a controlled environment, as shown in Figure 3.4. This kinematic video was used for observations.

In our experience, a hagfish in an aquarium prefers to be pressed up against the edges or touching other hagfishes rather than be alone in the center. This interesting behavioral characteristic, or *positive thigmotaxis*, was also observed in our experiment. Particularly, the tail exhibited the trait of positive thigmotaxis, which played a crucial role during all stages of knot formulation.

Except analyzing the photographs to measure bending limits, the rest of the experiments were exclusively done by our collaborators in the Department of Biology at Valodsta State University.

3.3.1 Rules for Knotting

Hagfish forms a knot using certain kinematic steps. The kinematic steps of knot formulations are as follows. First, the tail will form a loop by curving it to make a contact with a more anterior portion of the body. Then, the tail will follow the contour of the body surface in order to form one or several crossovers. Finally the tail will insert into a loop and the knot is formed. Haney organized these motion steps as (a) crossover, (b) tail wrap, and (c) tail insertion, which our simulation follows suit [6].

During this process, the key feature that they noticed is that as the hagfish slides the given knot anteriorly or posteriorly along the body, the constituent crossovers do not change in relation to each other. This was an essential feature for a hagfish to successfully form a knot, and motivated our idea of using positive thigmotaxis.

4. SIMULATOR*

4.1 Simulation Model

To model a hagfish, we use 100 rigid bodies and joints (Figure 4.1). Considering that a hagfish has a cartilaginous notocord, it may seem that using rigid bodies for the hagfish model is not appropriate. However, since the cartilaginous notocord is inextensible, using rigid bodies is still reasonable.

The rigid bodies and joints were aligned along the X-axis. The bodies were connected with X-revolute joints and YZ-universal joints in an alternating fashion, as shown in Figure 4.2. A revolute joint, or also called a hinge joint, has one degree of freedom, which rotates along a single axis. In the case of universal joints, they have two degrees of freedom. Since bodies and joints were aligned along X-axis, this allowed the joint to bend in Y-axis and Z-axis, but twisting along X-axis. We applied our twisting limit data to revolute joints, and bending limit data to universal joints. Applying the joint limit data would have been challenging using spherical joints.

4.2 Constraints

We reproduced the hagfish experiment video, by giving a set of constraints to our hagfish model. The constraints can be divided into two parts: bilateral constraints and unilateral constraints. Bilateral constraints are used to fix the hagfish head to the wall, and unilateral constraints are used for joint limits and contacts on the wall and self collisions. Figure 4.3 shows the visual reference of constraints. The red mark denotes the bilateral constraints, and the blue marks represent unilateral constraints.

We use forward Euler integration to advance the rigid bodies in time. We use different solvers, depending on the different types of constraints the model encountered.

*Reprinted by permission from Springer Nature Customer Service Center GmbH: Springer Nature, Bioinspired simulation of knotting hagfish [1], 2019. Copyright 2019 Springer Nature Switzerland AG.

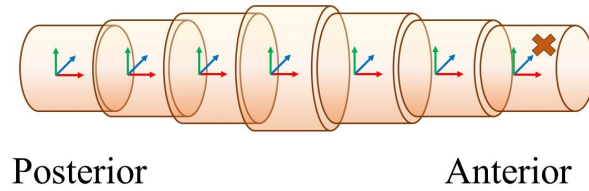


Figure 4.1: Hagfish model using rigid bodies [1].

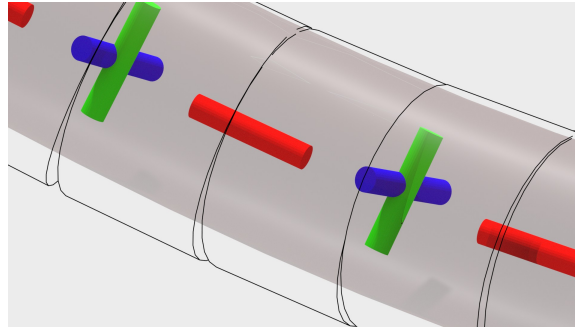


Figure 4.2: Hagfish bodies connected with revolute joints and universal joints [1].

4.2.1 No Constraints

If there are no constraints, we solve the following linear system:

$$M\dot{q} = M\dot{q}_0 + hf, \quad (4.1)$$

where M is the mass matrix, \dot{q} is the new velocity vector we are solving for, \dot{q}_0 is the velocity from the last time step, h is the fixed time step, and f is the force vector. Here, force includes all internal, external, and Coriolis forces. Once the velocities are computed, we update the positions as

$$q = q_0 + h\dot{q}. \quad (4.2)$$

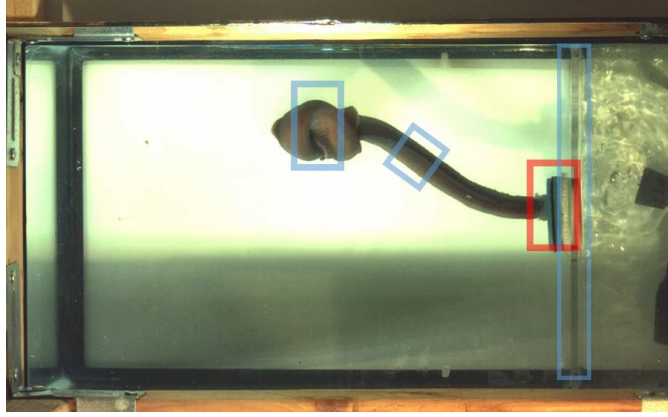


Figure 4.3: We use bilateral constraints to fix the head (red) and unilateral constraints for contact with the wall and itself (blue).

4.2.2 Only Bilateral Constraints

If there exist only bilateral constraints, we solve the problem using a Karush-Kuhn-Tucker (KKT) system [39]:

$$\begin{pmatrix} M & G^\top \\ G & 0 \end{pmatrix} \begin{pmatrix} \dot{q} \\ \lambda \end{pmatrix} = \begin{pmatrix} M\dot{q}_0 + hf \\ 0 \end{pmatrix}, \quad (4.3)$$

where G is the Jacobian of the bilateral constraints, and λ is the vector of Lagrange multipliers.

4.2.3 Bilateral and Unilateral Constraints

If there exist both bilateral and unilateral constraints, we solve the following quadratic program:

$$\begin{aligned} & \underset{\dot{q}}{\text{minimize}} && \frac{1}{2} \dot{q}^\top M \dot{q} - \dot{q}^\top (M\dot{q}_0 + hf) \\ & \text{subject to} && G\dot{q} = 0, \quad C\dot{q} \geq 0, \end{aligned} \quad (4.4)$$

where G and C each denotes the Jacobian matrices for bilateral and unilateral constraints. If the system drifts away from the constraint manifold due to constraints enforced at the velocity level, we stabilize the positions when necessary [40].

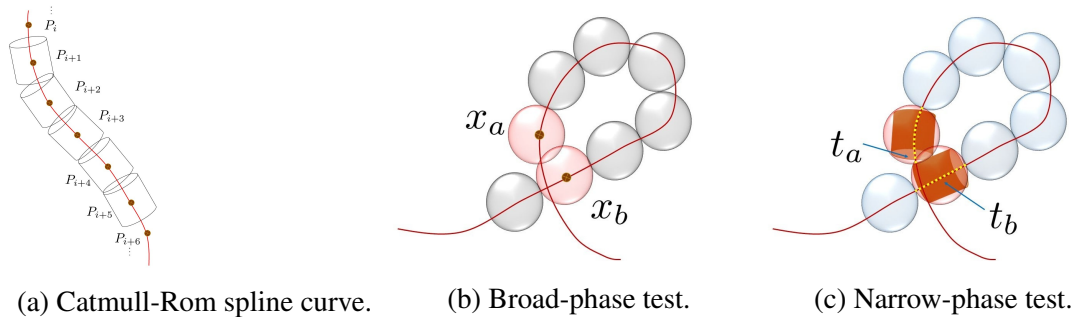


Figure 4.4: Contact handling [1].

4.3 Contact Handling

Due to the fact that we are using contact signals inspired by positive thigmotaxis, collision detection and contact handling are important aspects of our work. The contact handling steps are visually shown in Figure 4.4.

4.3.1 Collision Detection

In order to detect the colliding bodies, first we fit a Catmull-Rom spline curve passing through the center of each rigid body. This represents the cartilaginous notocord of the hagfish.

We create bounding spheres around the rigid bodies to perform broad-phase collision detection. If there is indeed a collision in broad-phase, we perform a narrow-phase test, using Newton's method to find the accurate colliding points on the potentially colliding bodies.

4.3.2 Newton's Method

When the bodies collide, we use Newton's method to compute the collision points. This is shown in Figure 4.4a. We use Newton's method to compute the root of the following function:

$$f(s_i, s_j) = \begin{pmatrix} x'(s_i)^\top (x(s_j) - x(s_i)) \\ x'(s_j)^\top (x(s_j) - x(s_i)) \end{pmatrix} = \begin{pmatrix} 0 \\ 0 \end{pmatrix}, \quad (4.5)$$

where s_i and s_j are spline parameters along the spline curve, $x(s_i)$ and $x(s_j)$ are positions along the curve, and $x'(s_i)$ and $x'(s_j)$ are the corresponding tangents, respectively.

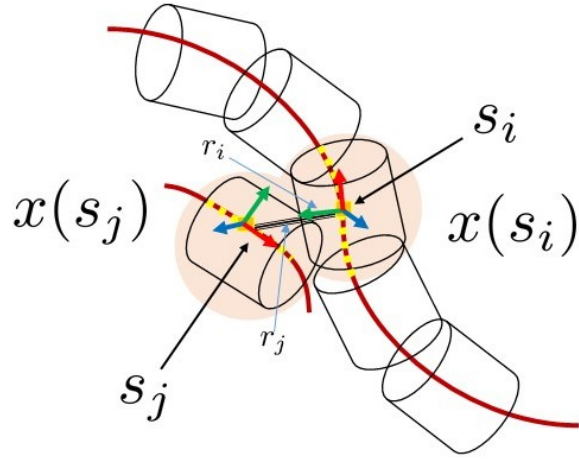


Figure 4.5: Newton's method [1].

Given that the spline parameters range from 0 to 1, we start our search from the middle, by setting initial parameters s_i and s_j both 0.5 before the search. Next we compute the colliding points by iteratively checking whether the tangents are orthogonal to the vector between the two positions (Equation 4.5), with a small tolerance threshold value.

These parameters are then used to compute colliding positions. Given that the radii of those two bodies are r_i and r_j , we compare the sum of the radii and the distance between $x(s_i)$ and $x(s_j)$ as the following equation.

$$\sqrt{(x(s_i) - x(s_j)) \cdot (x(s_i) - x(s_j))} < \sqrt{(r_i + r_j)^2} \quad (4.6)$$

If the distance between those two colliding positions is less than the sum of the radii of the two bodies (Equation 4.5), we can assume the narrow-phase collision has occurred. Thus we can successfully handle self contacts.

5. CONTROLLER*

The controller consists of two independent steps: forming the knot and sliding the knot. We use forward dynamics for forming the knot, and inverse dynamics for sliding the knot. Forward dynamics computes the motion based on the force, and inverse dynamics computes the force based on the motion.

5.1 Knot Forming

In order to form a knot, we use forward dynamics. We manually create a sequence of scripted forces. We use the aforementioned kinematic rules for knot formulation by Haney [6], which involves simple steps consisting of body crossover, tail wrap, and tail insertion. For each step, we apply forces on the terminal body of the hagfish model to achieve a desired motion, as shown in Figure 5.1. We found only linear forces were enough to produce a knot. This method is rather time consuming and requires effort, but it is very intuitive and fairly easy to achieve reasonable results. Figure 5.2 visually shows our knot forming process.

5.2 Knot Sliding Problem

Unlike knot forming, however, there is no intuitive way to apply forces or torques to make the knot slide. This can be easily found with a real world experiment, as we show in Figure 5.3.

In this small experiment, we used various kinds of flexible, pliant strings and formed a simple knot. Then we used a long rod, such as a pencil, placed it into the knot, and dragged the knot in the direction which we would like the knot to slide. For some strings, we added soap to reduce friction, to reproduce the smooth surface of hagfish.

What we discovered was that regardless of strings or added soap, it was a very hard problem to slide the knot even with a very flexible string with minimal friction. They either got stuck in the middle, or required an immense force, which often was tedious. This demonstrated that using

*Reprinted by permission from Springer Nature Customer Service Center GmbH: Springer Nature, Bioinspired simulation of knotting hagfish [1], 2019. Copyright 2019 Springer Nature Switzerland AG.

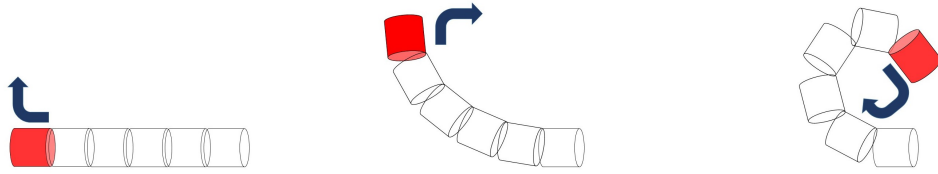


Figure 5.1: Force applied on the terminal body [1].



Figure 5.2: The knot forming steps [1].

scripted forces would not work well for the knot sliding problem.

5.2.1 Contact-Based Inverse Dynamics

Inspired by positive thigmotaxis, our contact-based inverse dynamics approach proved to be very effective for this problem.

Once we detect self collisions due to the knot formulation, we switch our controller from forward dynamics to inverse dynamics. As mentioned earlier, in inverse dynamics, we compute the forces and torques given a specified motion, and it can be cast as a constraint to be applied to the motion [30]. We name our constraint as the positive thigmotaxic constraint.

For self-collision points, we require that the projection of the relative velocity between the two contacting points onto the tangent direction to be greater than some value (Figure 5.4). Mathemat-



Figure 5.3: Real-world knot sliding experiment.

Table 5.1: Scalar parameter values for knot tightening and loosening [1]

Data	Values	Units
v_a, v_b (tightening, head)	0.0, 0.0	cm/s
v_a, v_b (tightening, tail)	0.5, 1.0	cm/s
v_a, v_b (loosening, head)	1.0, 1.0	cm/s
v_a, v_b (loosening, tail)	0.1, 1.0	cm/s

ically, this can be written as follows:

$$\begin{aligned}
 t_a^\top (\dot{x}_a - \dot{x}_b) &\geq v_a \\
 t_b^\top (\dot{x}_b - \dot{x}_a) &\geq v_b,
 \end{aligned} \tag{5.1}$$

where t_a and t_b are the unit tangent vectors of the colliding rigid bodies ($t = x'/\|x'\|$), \dot{x}_a and \dot{x}_b are the world velocities of the colliding points, and v_a and v_b are scalar parameters to control the sliding motion in tangential directions. These quantities can be computed as functions of the current generalized positions and velocities, q and \dot{q} [30]. We add our positive thigmotaxic constraint in the unilateral constraint matrix C .

5.2.1.1 Computations

Our approach may seem overly constrained and computationally expensive, because there exist many self-collisions during a knotting process, which consists of a large portion of the animal's

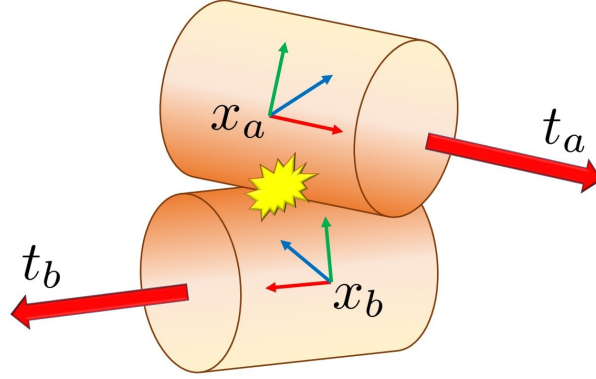


Figure 5.4: Visual representation of contact-based inverse dynamics [1].



Figure 5.5: Applying thigmotaxic constraints.

body.

However, in our approach, we do not apply thigmotaxic constraints to every colliding point. Instead, we sort the collisions by the parametric distance from the head, and apply the thigmotaxic constraints to only the first and the last collisions, as shown in red in Figure 5.5.

In order to take this approach, we need to keep the tail straight, which is different from the real-world hagfish video. If contacts are occurring in regions other than the knot itself, the sliding motion will not activate properly. However since our main focus is to find a method that enables knot sliding, rather than simply imitating the video, this is not a serious problem. Therefore, once the knot forms, we pull on the tail by applying a small force to the distal rigid body.

5.2.1.2 Knot Controls

With our approach, now we are able to control the knot by manipulating the scalar parameters of contact-based inverse dynamics in our method. In order to do this, we use two substeps: knot

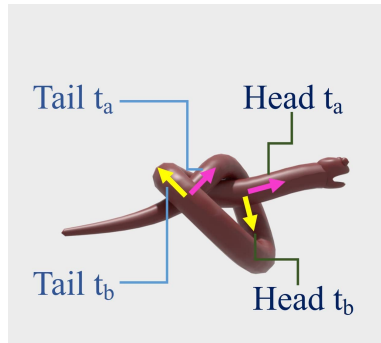


Figure 5.6: Thigmotaxic constraints for hagfish [1].



Figure 5.7: Knot tightening.



Figure 5.8: Knot loosening.

tightening and knot sliding.

First, we can use different scalar parameters to tighten or loosen the knot. Figure 5.7 and Figure 5.8 show two examples of how we can control the knots. In the first example, the tail parameters are given higher values to pull the tail out, resulting in knot tightening (Figure 5.7). On the other hand, in the second example, higher values are given to the head, for knot loosening (Figure 5.8). The scalar parameter values are given in Figure 5.6.

Once the knot is tightened sufficiently, we set the parameters to have the same values. This enables the knot to slide along its body toward the head effectively.

5.2.1.3 Positive Thigmotaxic Force

The forces computed by the inverse dynamics solver can be calculated with the Lagrange multipliers of the quadratic program. We divide the unilateral constraint Jacobian matrix C and Lagrange multiplier λ into three parts that correspond to joint limits, collisions, and thigmotaxis, as the following:

$$C = \begin{pmatrix} C_{\text{limits}} \\ C_{\text{collision}} \\ C_{\text{thigmo}} \end{pmatrix}, \quad \lambda = \begin{pmatrix} \lambda_{\text{limits}} \\ \lambda_{\text{collision}} \\ \lambda_{\text{thigmo}} \end{pmatrix}. \quad (5.2)$$

Then we compute the inverse dynamics force from positive thigmotaxis as follows:

$$f_{\text{thigmo}} = \frac{1}{h} C_{\text{thigmo}}^{\top} \lambda_{\text{thigmo}}. \quad (5.3)$$

6. RESULTS*

6.1 System Configuration

The simulator was implemented using C++, and the experiments were performed on a consumer desktop with an Intel Core i7-7600 CPU 3.6 Ghz and 16 GB of RAM. For numerical computations, we used Eigen for linear algebra, and Mosek for quadratic program.

6.2 Knot Sliding

Table 6.1 shows the biometric data of hagfish, and scalar parameters of our inverse sliding motion. Figure 6.1 visually compares the sliding motion between our simulation and the real hagfish, which is restrained in a custom tank. As can be seen, our method simulates the sliding motion of knot realistically.

The knot sliding motion steps were largely divided into three steps. First, we used manually scripted forces to make an initial knot. Next, we tightened the knot using the scalar parameters shown in Table 6.1. We use higher scalar parameters in the tail and set the 0 values in the head, so to pull the tail out from the knot with stronger drive. And lastly, using the tightened knot, we slid the knot along the body toward the head, by setting the head and tail parameters to be the same value. The resulting motion is smooth and effective.

6.3 Analysis of Force

We generated positive thigmotaxic forces using Equation 5.2, in X-axis, Y-axis, and Z-axis, respectively. Figure 6.2 shows the details, using the X-axis graph. The horizontal axis represents the indices of joints. Here, 0 denotes the joint in the head of the hagfish, and 50 denotes the tail. The diagonal axis shows the increase in time, following the direction of the arrow. The vertical axis denotes the positive thigmotaxic force, computed by our inverse dynamics controller. It can be seen how thigmotaxic force changes as the knot slides along the body toward the head. The

*Reprinted by permission from Springer Nature Customer Service Center GmbH: Springer Nature, Bioinspired simulation of knotting hagfish [1], 2019. Copyright 2019 Springer Nature Switzerland AG.

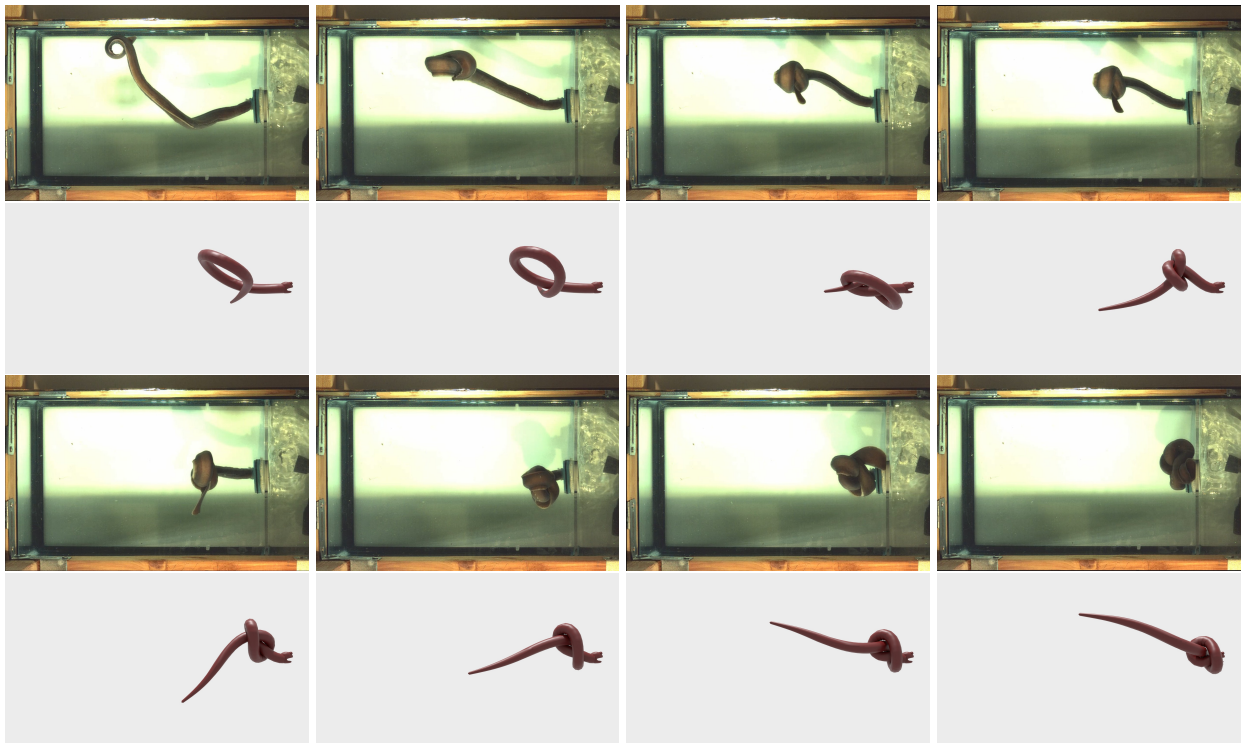


Figure 6.1: Comparison between our knotting hagfish with *positive thigmotaxis* and the actual hagfish video [1].

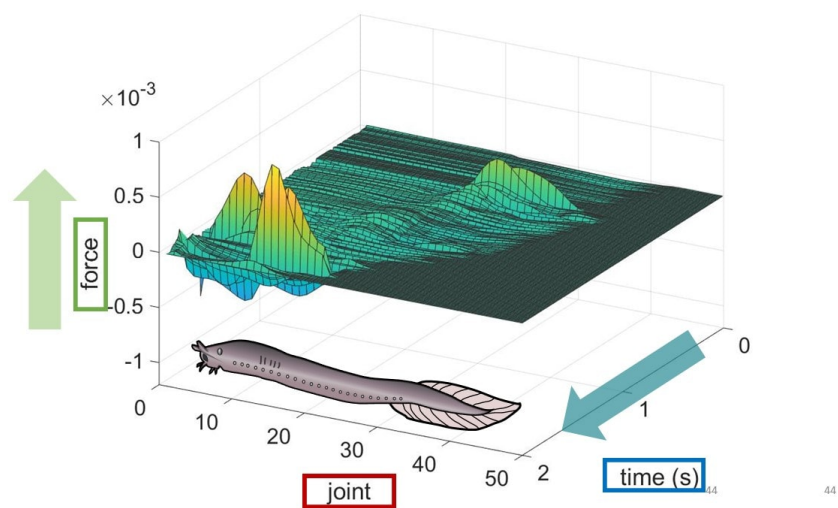


Figure 6.2: The visual representation of graph coordinates.

Table 6.1: Biometric data and inverse dynamics parameters [1].

Data	Values	Units
Length	42.4	cm
Mass	80	g
Circumference	5.6, 5.5, 5.6, 4.3	cm
Bending limit	21, 75, 45, 51	deg
Twisting limit	48	deg
v_a, v_b (tightening, head)	0.0, 0.0	cm/s
v_a, v_b (tightening, tail)	0.5, 2.0	cm/s
v_a, v_b (sliding, head)	2.0, 2.0	cm/s
v_a, v_b (sliding, tail)	2.0, 2.0	cm/s

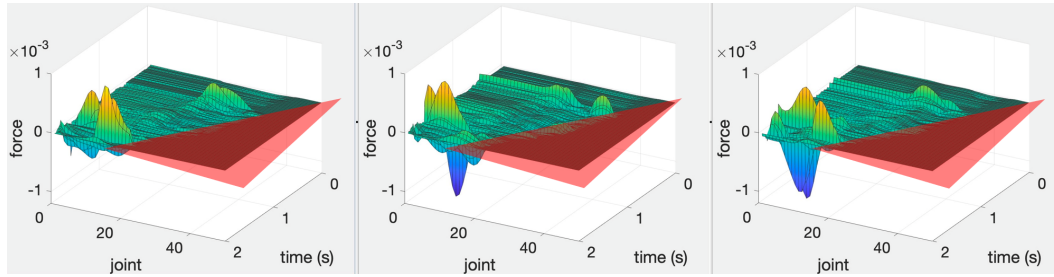


Figure 6.3: The thigmotaxic force becomes zero [1].

generated force looks quite noisy, but this is a typical case for inverse dynamics.

From the plot of the force, we have discovered several interesting traits. First, as the knot moves toward the head over time, the forces acting on the joints closer to the tail becomes zero (Figure 6.3). This is an expected result, because once the knot passes through the joint, that joint no longer needs to be controlled to move the knot. This trait can be seen in the red flat surface regions of each graph.

Second, more force is required when the knot approaches closer to the head, as shown by the yellow and blue regions in the graph. This is due to the fixation of head on the wall, which required moving the knot the whole length from the head to the tail. This is interesting, because we can extend our research to analyzing the retractile force that the hagfish knot is capable of. Biologists may gain further understanding on how hagfishes exploits its knot, for example, in feeding events.

Lastly, we have discovered that the forces rapidly change along the temporal dimension, but they are smooth in spatial dimension. This implies the possibility that control signals may be represented using a reduced set of basis, for example, using Fourier analysis, rather than exploiting every individual segments. This may be an important clue in discovering hagfish muscle controls on knot sliding motion.

7. CONCLUSION*

7.1 Contributions

In this thesis, we presented a simulation technique for knot sliding. This is called *contact-based inverse dynamics*, and it was cast as *positive thigmotaxic* constraints, named after the biological concept where we found the inspiration.

We have the following significant contributions. First, most of all, we have successfully implemented *positive thigmotaxis*, using our contact-based inverse dynamics. This allowed our hagfish model to slide the knot along the body, which none of the previous methods have achieved. Furthermore, we were able to adjust the knot, by tightening it or loosening it effectively. This ability would further our understanding in finding the mechanisms involved in knot controls and other application areas.

Second, we designed and implemented a simulator that generates results that are biologically realistic and informative. Hagfish commonly are found deep down in the oceans, and procurement process is costly. This hindered hagfish researchers from experimenting with hagfish more freely. Our simulator used the biometric data collected from a real world hagfish. We hope our work will enable researchers to use our simulator for testing out functional hypotheses of hagfishes.

Third, our simulation has potential for future applications, most notably, in soft-robotics. The difficult task that soft robots face today is in how to control flexible and pliant parts. We hope our work will aid in opening up a new horizon in this field. For example, using our knot sliding scheme combined with application of frictional contacts around the objects, robots could deliver items by surrounding the object with a body knot, and slide the knot through narrow spaces or areas that are difficult to reach by human hands or typical traditional rigid robots [35, 13, 17].

7.2 Future Work

There are several features that we would like to develop as our future work.

*Reprinted by permission from Springer Nature Customer Service Center GmbH: Springer Nature, Bioinspired simulation of knotting hagfish [1], 2019. Copyright 2019 Springer Nature Switzerland AG.

First, we would like to add contractile muscle fibers and use deformable flesh with continuum mechanics. In our current simulation, we used rigid bodies and simple skin mesh for our hagfish model. This agrees with hagfish trait, because hagfish body core can get quite stiff due to muscular hydrostats. Still, hagfish retain bodies and skin that can be relatively soft and deformable. By using muscle fibers and deformable flesh, we would be able to simulate a more realistic hagfish with further accurate contact geometry.

Second, from the results of inverse dynamics force, we have discovered that the forces in spatial dimensions are smooth. This implies that the activations in control signals can be represented using a reduced basis. This is an important clue for our future work, for it implies we may find the hagfish muscle controls during sliding the knot.

Third, so far, we have focused on forming the simplest overhand knot for sliding. However, in reality, it has been observed that hagfish are capable of forming more complex knots, such as figure-8, or Miller-Institute knots. We would like to manipulate different kinds of knots for sliding, to further understand the knot controls.

Lastly, we would like to tie the initial knot by using control signals. Currently, we are using scripted forces to formulate an initial knot. Although this is intuitive and easy to achieve a desired motion, it is not only time consuming and takes a lot of effort, but it doesn't fully represent the knot formulation of real-world hagfish.

REFERENCES

- [1] Y. Hwang, T. A. Uyeno, and S. Sueda, “Bioinspired simulation of knotting hagfish,” *Springer*, vol. 11844, pp. 75–86, October 2019.
- [2] H. Adam, “Different types of body movement in the hagfish, *myxine glutinosa* l,” *Nature*, vol. 188, no. 4750, pp. 595–596, 1960.
- [3] R. Strahan, “The behaviour of myxinoids,” *Acta Zoologica*, vol. 44, no. 1, pp. 73–102, 1963.
- [4] V. Zintzen, C. D. Roberts, M. J. Anderson, A. L. Stewart, C. D. Struthers, and E. S. Harvey, “Hagfish predatory behaviour and slime defence mechanism,” *Scientific Reports*, vol. 1, p. 131, 2011.
- [5] A. J. Clark and A. Summers, *Ontogenetic scaling of the morphology and biomechanics of the feeding apparatus in the Pacific hagfish *Eptatretus stoutii**, vol. 80. *Journal of Fish Biology*, 2012.
- [6] W. A. Haney, “Characterization of body knotting behavior in hagfish,” Master’s thesis, Valdosta State University, May 2017.
- [7] B. L. Clubb, A. J. Clark, and T. A. Uyeno, “Powering the hagfish “bite”: the functional morphology of the retractor complex of two hagfish feeding apparatuses,” *Journal of morphology*, vol. 280, no. 6, pp. 827–840, 2019.
- [8] T. A. Uyeno and A. J. Clark, “Muscle articulations: flexible jaw joints made of soft tissues,” *Integrative and comparative biology*, vol. 55, no. 2, pp. 193–204, 2015.
- [9] A. W. Haney, A. J. Clark, and T. A. Uyeno, “Characterization of body knotting behavior used for escape in a diversity of hagfishes,” *Journal of Zoology*, 2019. in press.

- [10] J. H. Long, M. Koob-Emunds, B. Sinwell, and T. J. Koob, “The notochord of hagfish *myxine glutinosa*: visco-elastic properties and mechanical functions during steady swimming,” *Journal of Experimental Biology*, vol. 205, no. 24, pp. 3819–3831, 2002.
- [11] W. Andrew and C. P. Hickman, *Histology of the vertebrates: a comparative text*. Saint Louis: Mosby, 1974.
- [12] A. J. Clark, C. H. Crawford, B. D. King, A. M. Demas, and T. A. Uyeno, “Material properties of hagfish skin, with insights into knotting behaviors,” *The Biological Bulletin*, vol. 230, no. 3, pp. 243–256, 2016.
- [13] D. Trivedi, C. D. Rahn, W. M. Kier, and I. D. Walker, “Soft robotics: Biological inspiration, state of the art, and future research,” *Applied Bionics and Biomechanics*, vol. 5, no. 3, pp. 99–117, 2008.
- [14] I. Vladu, D. Străombeanu, M. IvĂnescu, N. BĂozdoacĂ, C. Vladu, and M. Florescu, “Control system for a hyper-redundant robot,” *IFAC Proceedings Volumes*, vol. 45, no. 6, pp. 853–858, 2012.
- [15] F. H. Martini, *The Ecology of Hagfishes*, pp. 57–77. Springer Netherlands, 1998.
- [16] J. W. Alexander and G. B. Briggs, “On types of knotted curves,” *Annals of Mathematics*, vol. 28, no. 1/4, pp. 562–586, 1926.
- [17] D. Rus and M. T. Tolley, “Design, fabrication and control of soft robots,” *Nature*, vol. 521, no. 7553, p. 467, 2015.
- [18] E. Evans, Y. Hwang, S. Sueda, and T. A. Uyeno, “Estimating whole body flexibility in pacific hagfish,” in *The Society for Integrative & Comparative Biology*, January 3-7 2018.
- [19] M. Bergou, M. Wardetzky, S. Robinson, B. Audoly, and E. Grinspun, “Discrete elastic rods,” *ACM Trans. Graph.*, vol. 27, pp. 63:1–63:12, Aug. 2008.

- [20] F. Bertails, B. Audoly, M.-P. Cani, B. Querleux, F. Leroy, and J.-L. Lévêque, “Super-helices for predicting the dynamics of natural hair,” *ACM Trans. Graph.*, vol. 25, pp. 1180–1187, July 2006.
- [21] C. Deul, T. Kugelstadt, M. Weiler, and J. Bender, “Direct position-based solver for stiff rods,” *Computer Graphics Forum*, vol. 37, no. 6, pp. 313–324, 2018.
- [22] R. Featherstone, “The calculation of robot dynamics using articulated-body inertias,” *INT J ROBOT RES*, vol. 2, no. 1, pp. 13–30, 1983.
- [23] D. K. Pai, “Strands: Interactive simulation of thin solids using cosserat models,” *Computer Graphics Forum*, vol. 21, no. 3, pp. 347–352, 2002.
- [24] S. Sueda, G. L. Jones, D. I. W. Levin, and D. K. Pai, “Large-scale dynamic simulation of highly constrained strands,” *ACM Trans. Graph.*, vol. 30, pp. 39:1–39:10, July 2011.
- [25] D. Baraff, “Fast contact force computation for nonpenetrating rigid bodies,” in *Proceedings of the 21st Annual Conference on Computer Graphics and Interactive Techniques, SIGGRAPH ’94*, (New York, NY, USA), pp. 23–34, ACM, 1994.
- [26] S. Jain and C. K. Liu, “Controlling physics-based characters using soft contacts,” *ACM Trans. Graph.*, vol. 30, pp. 163:1–163:10, Dec. 2011.
- [27] J. Kim and N. S. Pollard, “Fast simulation of skeleton-driven deformable body characters,” *ACM Trans. Graph.*, vol. 30, no. 5, pp. 1–19, 2011.
- [28] L. Liu, K. Yin, B. Wang, and B. Guo, “Simulation and control of skeleton-driven soft body characters,” *ACM Trans. Graph.*, vol. 32, no. 6, pp. 1–8, 2013.
- [29] T. Shinar, C. Schroeder, and R. Fedkiw, “Two-way coupling of rigid and deformable bodies,” in *Proc. SCA 2008*, pp. 95–103, 2008.
- [30] Y. Wang, N. J. Weidner, M. A. Baxter, Y. Hwang, D. M. Kaufman, and S. Sueda, “RED-MAX: Efficient & flexible approach for articulated dynamics,” *ACM Transactions on Graphics*, vol. 38, pp. 104:1–104:10, July 2019.

- [31] D. M. Kaufman, S. Sueda, D. L. James, and D. K. Pai, “Staggered projections for frictional contact in multibody systems,” *ACM Trans. Graph.*, vol. 27, pp. 164:1–164:11, Dec. 2008.
- [32] J. Phillips, A. Ladd, and L. E. Kavraki, “Simulated knot tying,” in *IEEE Int. Conf. Robot. Autom.*, vol. 1, pp. 841–846, IEEE, 2002.
- [33] J. Brown, J.-C. Latombe, and K. Montgomery, “Real-time knot-tying simulation,” *Vis. Comput.*, vol. 20, pp. 165–179, May 2004.
- [34] G. Sumbre, G. Fiorito, T. Flash, and B. Hochner, “Octopuses use a human-like strategy to control precise point-to-point arm movements,” *Current biology : CB*, vol. 16, pp. 767–72, 05 2006.
- [35] N. Simaan, “Snake-like units using flexible backbones and actuation redundancy for enhanced miniaturization,” in *Proc. ICRA 2005*, pp. 3012–3017, April 2005.
- [36] D. G. Thelen and F. C. Anderson, “Using computed muscle control to generate forward dynamic simulations of human walking from experimental data,” *Journal of biomechanics*, vol. 39, no. 6, pp. 1107–1115, 2006.
- [37] Y. Lee, M. S. Park, T. Kwon, and J. Lee, “Locomotion control for many-muscle humanoids,” *ACM Trans. Graph.*, vol. 33, pp. 218:1–218:11, Nov. 2014.
- [38] S. Sueda, A. Kaufman, and D. K. Pai, “Musculotendon simulation for hand animation,” *ACM Trans. Graph.*, vol. 27, pp. 83:1–83:8, Aug. 2008.
- [39] S. Boyd and L. Vandenberghe, *Convex Optimization*. Cambridge University Press, 2004.
- [40] J. Baumgarte, “Stabilization of constraints and integrals of motion in dynamical systems,” *Comput. Methods in Appl. Mech. Eng.*, vol. 1, pp. 1–16, Jun 1972.